

Integrated Switch Current Sensor for Shortcircuit Protection and Current Control of 1.7-kV SiC MOSFET Modules

Jun Wang, Zhiyu Shen, Rolando Burgos, Dushan Boroyevich
Center for Power Electronics Systems
Virginia Polytechnic Institute and State
Blacksburg, VA 24061, USA
junwang@vt.edu

Abstract—This paper presents design and implementations of a switch current sensor based on Rogowski coils. The current sensor is designed to address the issue of using desaturation circuit to protect the SiC MOSFET during shortcircuit. Specifications are given to meet the application requirement for SiC MOSFETs. It is also designed for high accuracy and high bandwidth for converter current control. PCB-based winding and shielding layout is proposed to minimize the noises caused by the high dv/dt at switching. The coil on PCB are modeled by impedance measurement, thus the bandwidth of coil is calculated. At the end, various test results are demonstrated to validate the great performance of the switch current sensor.

Keywords—current sensing; Rogowski; SiC MOSFET; shortcircuit; current control

I. INTRODUCTION

SiC MOSFET, as a wide-bandgap device, has superior performance for its high breakdown electric field, low on-state resistance, fast switching speed and high working temperature [1]. High switching speed enables high switching frequency, which improves the power density of high power converters. The gradual cost reduction and packaging advancement bring a promising trend of replacing the conventional Si IGBTs with SiC MOSFET modules in high power applications.

Shortcircuit protection is one of the major challenges preventing this from happening. [2] analyzed the necessity of introducing new shortcircuit protection method for SiC MOSFET, compared to the conventional desaturation (DeSat) method. The main reason is about the different characteristics between MOSFET and IGBT. Fig. 1 shows the output characteristics of specific commercial Si IGBT and SiC MOSFET modules with the same voltage (1700V) and current ratings (225A@~100°C). The IGBT curves present a “hard” turning point between the transistor’s saturation and linear region. The current almost doesn’t increase and the voltage rises dramatically. The junction temperature of the IGBT doesn’t cast too much influence on the current difference for a given collector-emitter voltage V_{CE} . All those characteristics make the “DeSat” perfectly suit for the IGBT shortcircuit protection. When shortcircuit occurs, the collector current rises very

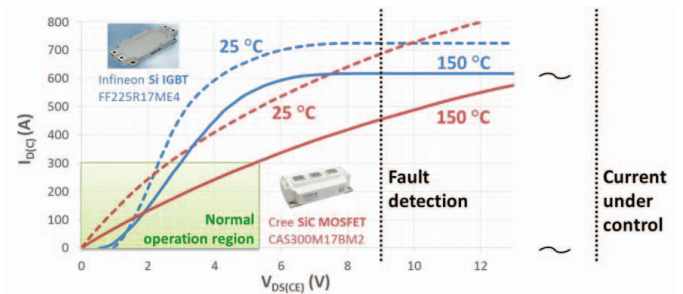


Fig. 1. Output characteristics comparison: Si IGBT vs. SiC MOSFET

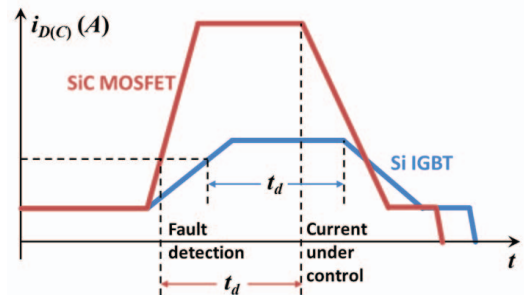


Fig. 2. Principle shortcircuit current comparison: Si IGBT vs. SiC MOSFET

quickly and reaches its saturation value, where the V_{CE} hits the protection threshold value (“Fault detection” in the Fig.1). Despite that a delay t_d always exists between the fault detection and the time when fault current is under control, the IGBT current is maintained and doesn’t become higher. The IGBT device is usually designed to be able to withstand high shortcircuit current for 10~15 μ s, which is sufficient for the device to turn off safely. Sensing errors may be induced by the junction temperature variation, but they are tolerable and not large enough to cause false triggering of the protection.

On the other hand, the output characteristics of the SiC MOSFET are “softer” in a wide current region. Fig.1 shows that the current keeps rising as the drain current I_C and drain-source voltage V_{DS} are at high values. In the time domain, in Fig.2, during the DeSat protection delay t_d , the MOSFET drain current will increase dramatically at shortcircuit. The accumulated energy on the SiC MOSFET will extensively

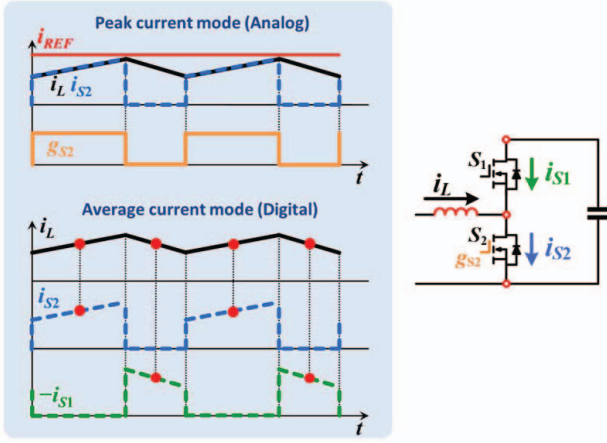


Fig. 3. Current sensing for converter control

exceed that of the IGBTs. Accordingly the MOSFET may not survive for a long delay time. The DeSat requires blanking time to ensure that the device has been fully turned on. The ringing at the fast turn-on of SiC MOSFETs demands even longer blanking time than the Si IGBTs, which further extends the delay time t_d , and thus elevate the current peak at shortcircuit. The temperature dependency of the MOSFET output characteristics is another issue presented in Fig.1, which indicates significant current threshold variation with a fixed V_{DS} at different converter conditions. This may lead to ineffective protection at the start-up of the converter. Last but not the least, the parasitic capacitance of the DeSat blocking diode can bring high ringing current to the circuit when the device is switching at very high dv/dt .

The abovementioned analysis shows that DeSat protection does not suit for the SiC MOSFET modules. Direct measurement of the device current can be a better solution as long as the switch current sensor can provide large enough bandwidth (BW), low response delay and fair accuracy. Rogowski coil used as a switch current sensor was implemented as early as 1990s [3] for motor drive phase current sensing, where the main switching devices were Si IGBTs. It was also used for current sharing of paralleled IGBTs and demonstrated good performance [4]. However, the switch current sensor was not widely adopted for Si IGBT shortcircuit protection as the DeSat is a simpler and more cost-effective solution. [2][5] shows an implementation where Rogowski coil-based switch current sensor is used for shortcircuit protection of the SiC MOSFET modules. In this paper, the sensor is integrated together with gate driver on the same board.

This paper also designs the sensor for high accuracy targeting at current control. As shown in Fig.3, fundamentally, the switch current carries all necessary information for inductor current control of a general converter. In the analog peak-current mode control, i_{S2} carries the ramp information of the inductor current for the touch-and-switch-off action. This is particularly useful for the control method proposed in [6]-[8]. In the digital average-current mode, the averaged inductor current is obtained by sampling at the middle point of on-state of either i_{S1} or i_{S2} . [3] shows an op-amp adder circuit to directly

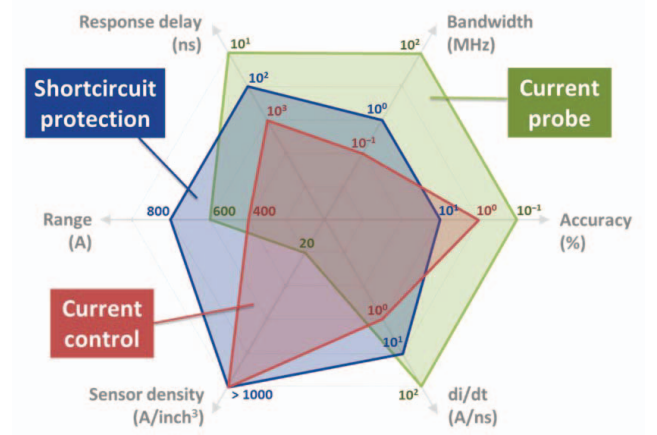


Fig. 4. Performance comparison of current measurement solutions

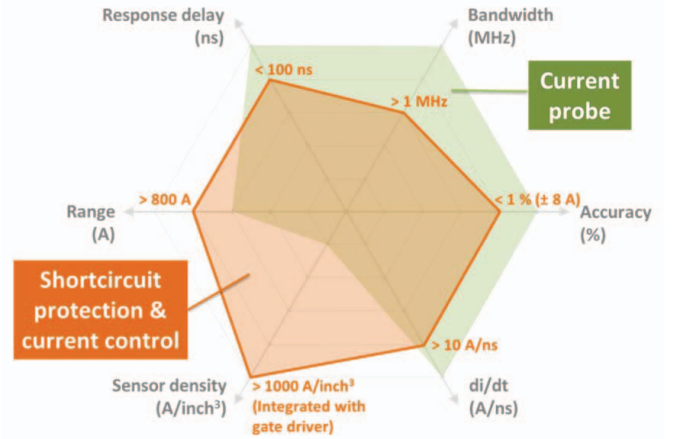


Fig. 5. Specifications of the switch current sensor

generate the analog inductor current. Therefore, the switch current provide more than enough information for current control. The excessive information can be used as sensor redundancy where higher reliability is brought. In medium voltage applications where Power Electronics Building Block (PEBB) based converters or multilevel converter are wide used [9][10], switch current sensor can ease the diagnostics of damaged device, or help monitoring abnormal devices. However, challenges do exist mainly due to the high dv/dt and the non-ideal performance of the integrator. The solutions and results are presented in this paper.

II. REQUIREMENT, SPECIFICATIONS, FUNDAMENTALS, AND CHALLENGES OF THE CURRENT SENSOR

A. Requirement and specifications

In order to sense currents for different purposes regarding the SiC MOSFET modules, Fig.4 shows the different requirements in the aspects of range, response delay, bandwidth, accuracy, di/dt , and sensor density. Shortcircuit protection requires the highest measurement range. The relatively high BW, di/dt and short response delay are also necessary to achieve fast protection. Further, protection sensor can tolerate 10% inaccurate error in practical applications. The sensor for current control requires higher accuracy than the protective one, but in other aspects the latter should have

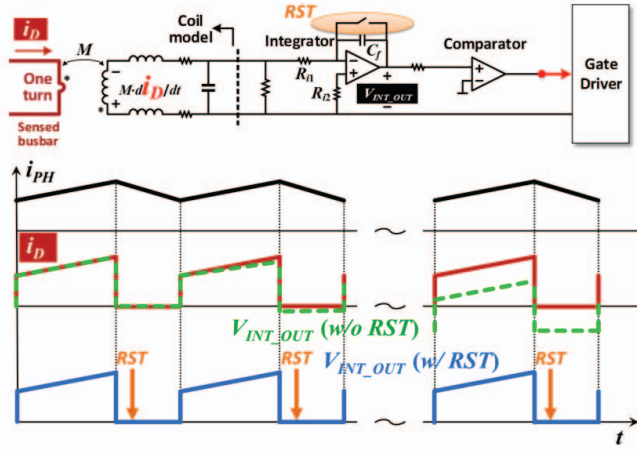


Fig. 6. Fundamentals of the switch current sensor

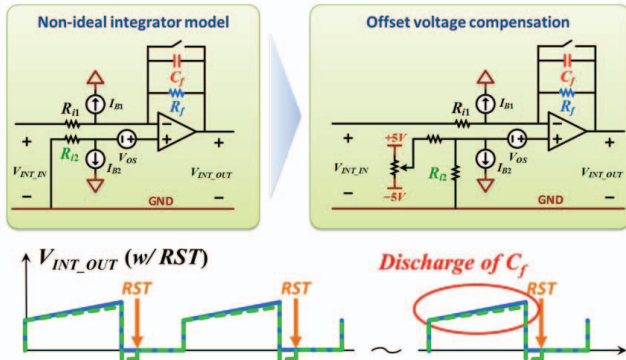


Fig. 8. Non-ideal integrator and compensation circuit

superior performances. The current probe for test and validation requires the highest performances in almost all the respects. In terms of the sensor density, a commercial Rogowski probe has a value of 20 A/inch³, which is too low to be affordable for a power converter. In this design it is required a density of 1000 A/inch³ for the protection and control sensor, which brings higher converter power density.

Combining the requirement for both the shortcircuit protection and converter control, the specifications of the current sensor in this paper is defined as in Fig.5. By sacrificing the performance in response delay, BW, accuracy, di/dt, the switch current sensor is able to be integrated into a gate driver board when still meeting all the requirements.

B. Fundamentals

The switch current sensor basically comprise of a Rogowski coil and an integrator. The Rogowski coil serves as a differentiator that generates di/dt value of the sensed current, scaled by a factor of the mutual inductance between the sensed busbar and the coil. The integrator work together with the coil to convert the di/dt information back to the current information. Either passive or active integrator can be selected [11], and in general the latter one has higher BW but requests more complex circuitry. In reality an ideal integrator with infinite gain at zero frequency does not exist. The operation waveforms of the switch current sensor illustrate the

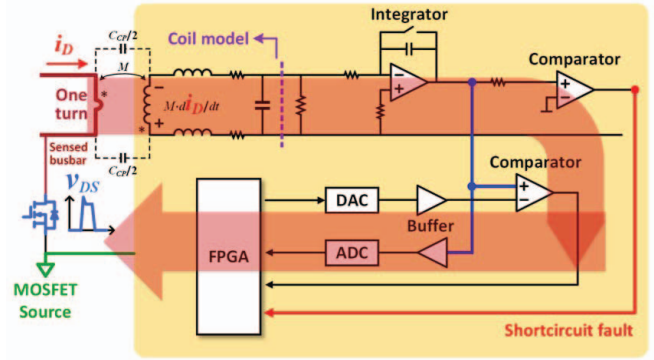


Fig. 9. Dv/dt issue of the switch current sensor

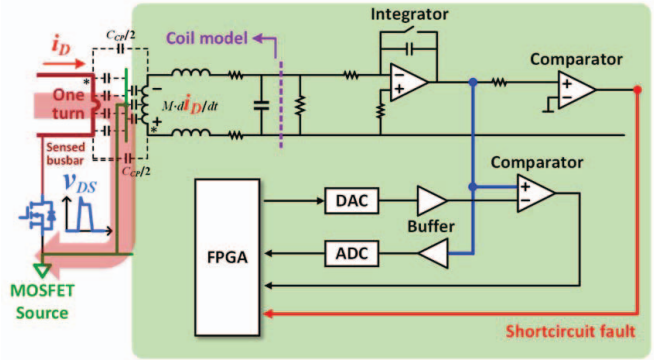


Fig. 10. Shield path to bypass the common-mode noise

phenomenon in Fig.6. The red waveform is the drain current i_D and the green one is the sensor output without a reset circuit. At steady state the mean value of the green waveform will be a finite constant due to the non-ideal integrator, which is usually designed to be zero as a commercial Rogowski probe does. The green waveform cannot be used for either protection or control because the real amplitude of the drain current cannot be correctly sensed. To resolve the problem, a reset switch is added to the integrator to reset the output to zero when the SiC MOSFET is switched off, shown in the blue waveform. Eventually the switch current sensor can sense pulsating current with correct amplitude. The ideal transfer gain from the sensed current to the sensor output voltage is given in (1).

$$G_{\text{SENSOR}} = M / (R_1 \cdot C_f) \quad (1)$$

C. Challenges

The main challenges in this design work for a high-accuracy high-BW switch current sensor include the non-ideal performance of the integrator and the noise immunity at high dv/dt. The first challenge is illustrated as in Fig.8. With the reset switch added to the integrator, the ideal sensor output should be the same as the blue waveform, though, in practice, it will be a non-zero offset voltage during the off-state of the SiC MOSFET. This is caused by the bias current and the offset voltage of the non-ideal operational amplifier (Op-Amp) (Left, Fig.8). The offset value is determined by the R_1 , R_2 and R_f . Most of the Op-Amp is designed to have trivial bias current mismatch between the inverting and non-inverting terminals, nonetheless, the offset voltage V_{OS} is inevitably about 10 mV.

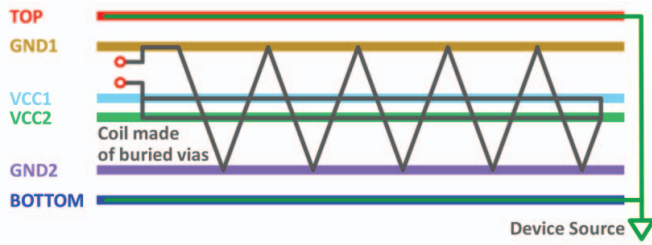


Fig. 11. Rogowski coil design on 6-layer PCB

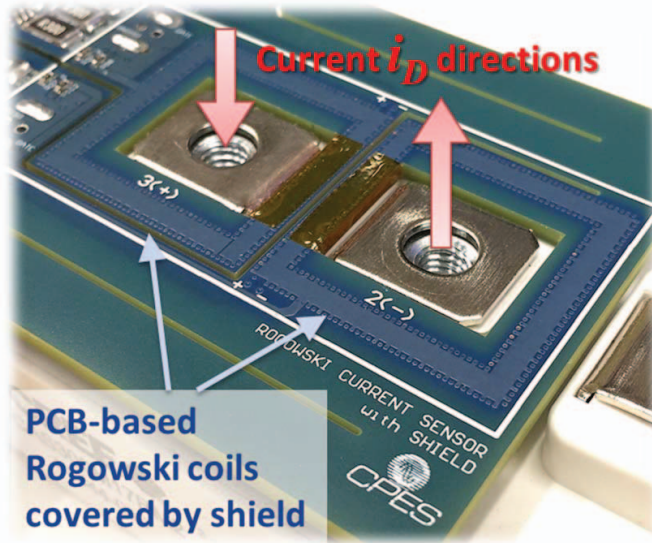


Fig. 12. Final layout of the Rogowski coils with shield

The offset voltage will be scaled by R_f/R_D , giving a few volts offset or even saturation at the output.

This issue can be resolved by a basic offset compensation circuit shown in the right-hand side of the figure. Even with both reset switch and the offset compensation, the integration capacitor can still be slowly discharged by the R_f or any Op-Amp load resistors. The R_f can be neither overlarge to make the offset compensation difficult, nor oversmall to discharge C_f very fast. The output waveform with quickly discharged C_f is depicted as the green waveform in Fig.8. As a result, for a given design parameter, there will be limitation for the maximum length of an on-state switching pulse of a PWM circuit, which is usually a limit for the switching period.

The fast switching speed of the medium-voltage SiC MOSFET brings the other challenge. Fig. 9 shows the principle circuit diagram of the high-side switch current sensor. The positive busbar is usually the high-side device terminal that can be implemented with Rogowski coils. The ground of the sensing circuit has to be connected to the source of the SiC MOSFET to turn-off the device with the shortest delay as soon as a shortcircuit occurs. The switching v_{DS} is placed on the parasitic coupling capacitance between the sensed busbar and sensor ground, thus a common-mode current (CM) will flow through the signal and the ground traces. The maximum dv/dt can reach as high as 30 V/ns. With a 2-pF coupling capacitance, the noise current can be as high as 60 mA with frequency at megahertz. When this current flow through the

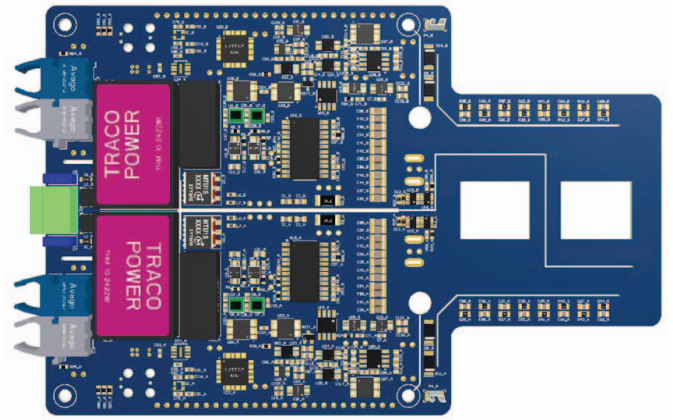


Fig. 13. 3D-layout of the gate driver board with integrated sensors

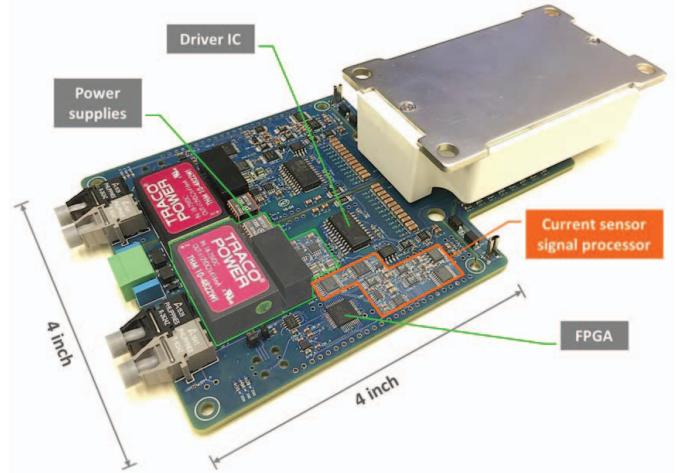


Fig. 14. Prototype of the gate driver board with integrated sensors

asymmetric signal and ground traces (both with winding inductance), a differential noise voltage will be generated at the input of the integrator, so that the accuracy will be reduced.

To overcome this challenge, a PCB-based shield is implemented as shown in Fig.10 to bypass most of the noise current through the shield trace. The coupling capacitance C_{CP} between the sensed busbar and the Rogowski coil is simulated to be reduced by 96%. However, this solution brings about another issue that the added coupling capacitance between the shield and the coil will generate another resonant frequency that decrease the BW of the current sensor.

III. LAYOUT DESIGN AND LIMITATIONS OF THE SENSORS

A. Layout design

The layout of the Rogowski coils is designed on a 6-layer PCB as shown in Fig.11. The top and bottom layer are used to construct the shield. Numerous single ended vias are placed from the top to the bottom layer to form a shield wall without creating eddy current loops, which can be observed in Fig.12. The winding are designed in the four internal layers. The second layer and the fifth is used to construct the multi-turn windings and the third and the forth layer are used to form the single-turn compensation winding.

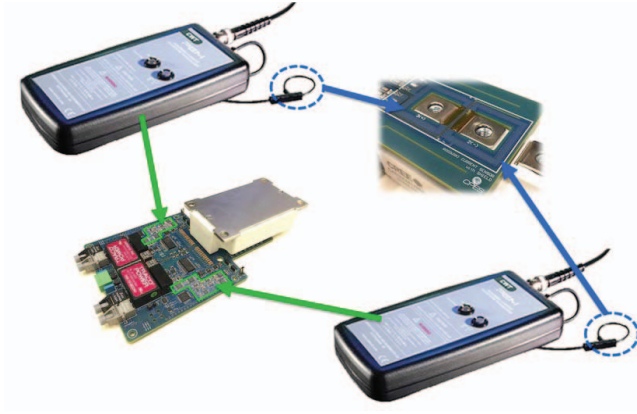


Fig. 15. Current sensor density improvement

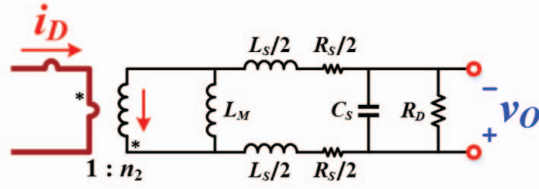


Fig. 16. Equivalent circuit model of the Rogowski coil without shield

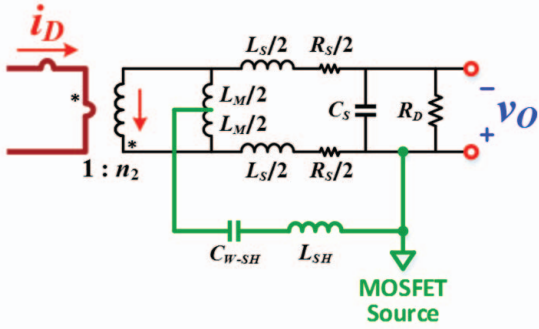


Fig. 17. Equivalent circuit model of the Rogowski coil with shield

Fig.13 shows the 3D layout of the gate driver board with a clear overview of the installation through holes and the signal processing components. In Fig.14, the power supplies, driver IC and the FPGA layout are also presented in addition to the sensor signal processing components, which includes the Op-Amps, comparators, reset switch. ADC and DAC converters for control purposes are included as well. The principle circuit diagram of the ADC and DAC has been shown in Fig. 10. The ADC is used to convert the analog sensor output to a digital signal for digital control. The DAC is used to generate an analog reference for the peak-current mode control as depicted in Fig.3.

The design actually integrates two Rogowski probes into one gate driver board, extending its accurate measurement range to pulsating current with DC offset. As shown in Fig.15, more than 50x improvement of the sensor density has been achieved. The cost is also reduced due to the shared PCB by both the gate driver and the sensor.

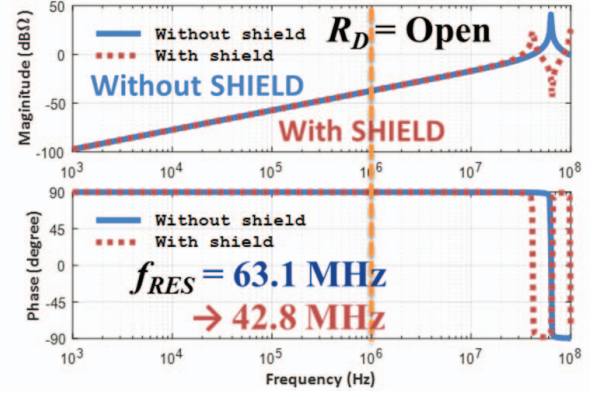


Fig. 18. Transfer impedance from i_D to v_O , with R_D open

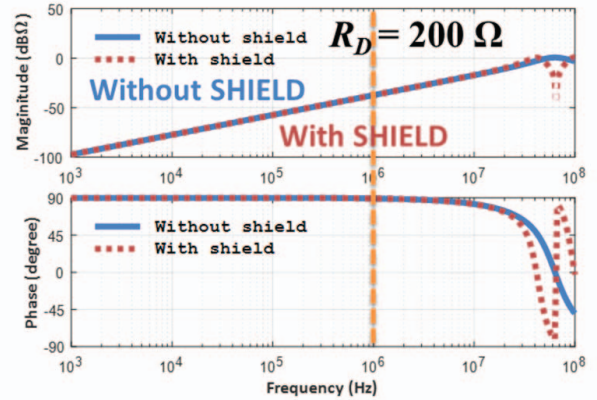


Fig. 19. Transfer impedance from i_D to v_O , with $R_D=200\ \Omega$

B. Limitations

The switch current sensor hold two main application limitations because of its fundamentals. Firstly, the sensor cannot correctly measure device currents without periodical off-state that should be longer than minimum length. The length is determined by the dead-time and the reset constant of the integrator. For applications where the device is not switching but the current flowing through it is still pulsating, the switching current sensor possibly works. Secondly, because of the discharge of the integration capacitor, the sensor accuracy cannot be guaranteed if the conduction-state pulse exceed the maximum length. This behavior usually limits the minimum switching frequency when implementing the switch current sensor, which in this case is designed to be 500 Hz.

IV. EXPERIMENTAL VALIDATIONS

A. Impedance measurement for BW estimation

Equivalent circuit models of the Rogowski coil with and without the shield path are shown in Fig.16 and Fig.17. All the component parameters are measured and calculated with an impedance analyzer. Then the bode plot of the transfer impedance from i_D to v_O are shown in Fig.18 and Fig.19 with different damping resistance R_D . In Fig.18, it can be observed that the shield reduces the first resonant frequency from 63.1 MHz to 42.8 MHz mainly because of the induced parasitic

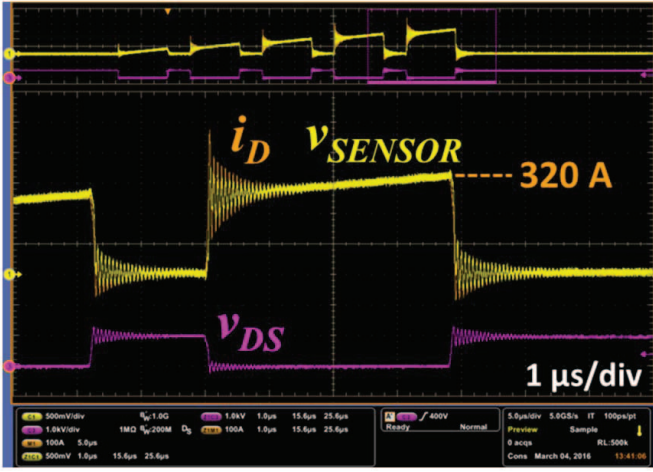


Fig. 20. Sensor performance at 5-pulse tests, for protection

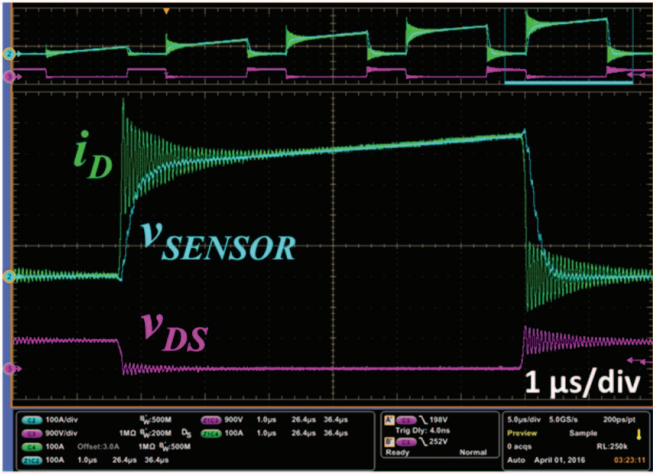


Fig. 21. Sensor performance at 5-pulse test, for control

capacitance C_{W-SH} from winding to shield. Fig.19 shows what with proper damping, the resonant peaks are reduced but the gain at 1 MHz is good with +20 dB/dec slope and without phase delay.

B. Sensor performance test

The sensor performance has been validated in various tests. Fig.20 shows the sensor performance at a 5-pulse test measuring SiC MOSFET drain current from 64 A to 320A with DC bus voltage to be 1 kV. This sensor output is used for protection purpose. It can be observed that the magnitude of the sensor output (yellow) match the Rogowski probe CWT-3B waveform (orange) very well at steady state. The ringing magnitude has been filtered to prevent false protection triggering at the hard turn-on of the SiC MOSFET. Fig. 21 shows the further filtered waveform of the sensor output. The switching ripples are completely eliminated and this signal is good for current mode control. The measurement error is less than 1% at the steady state.

Overcurrent protection test has been done to validate the protection performances, in Fig.22 and Fig.23. In this test, both the soft protection and the hard protection of the gate driver IC

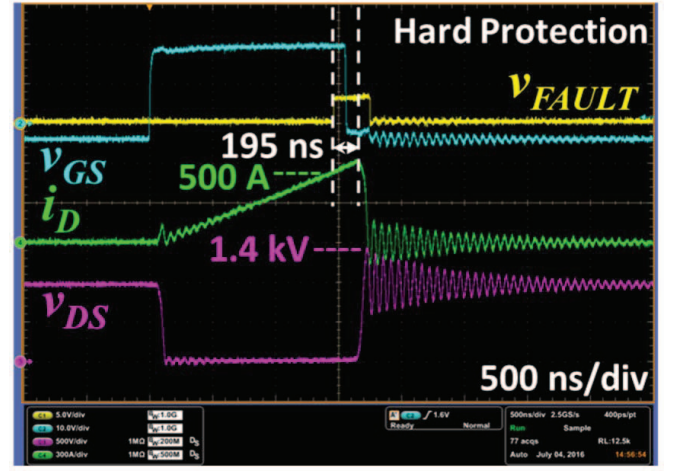


Fig. 22. Overcurrent protection test, hard protection

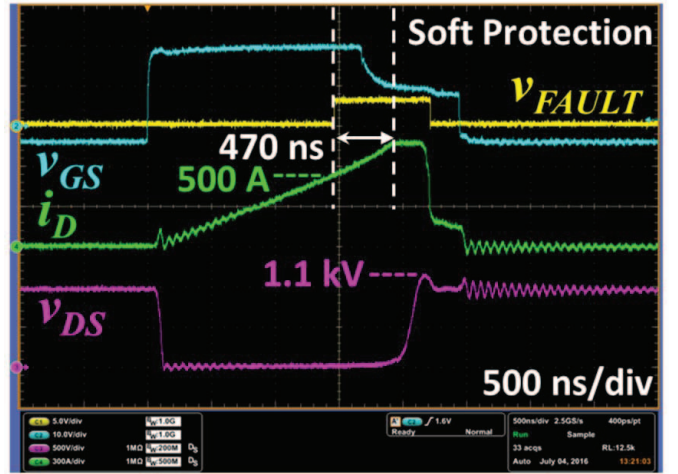


Fig. 23. Overcurrent protection test, soft protection

STMicro STGAP1S is evaluated. It is observed that as soon as the drain current exceed 500-A threshold value within 1.5 μs, the comparator output v_{FAULT} is set high and the protection has been activated in the driver IC. The hard protection only takes 195 ns response delay between the fault detection and current drop, with 1.4 kV turn-off voltage spike induced (Fig.22). The soft protection takes 470 ns delay, and induces 1.1 kV turn-off voltage spike (Fig.23). These protection test results show that the current sensor is able to achieve overcurrent protection at very short delay with high noise immunity.

Continuous test has also been operated to validate the sensor performance for control. Fig.24 shows a Quasi-Square-Wave mode operation of the converter where zero voltage turn-off of the SiC MOSFET is achieved. The sensor output (yellow) also follows the probe current very well from zero to the magnitude. Fig.25 shows the ADC digital signals sampling at 2 MHz under the same continuous operation condition. Both the clock and data are not influenced by the switching noises even at switching transients. Finally, the digital data has been converted to decimal values in Matlab. Fig.26 shows the digital result matches very well with the probe waveform.

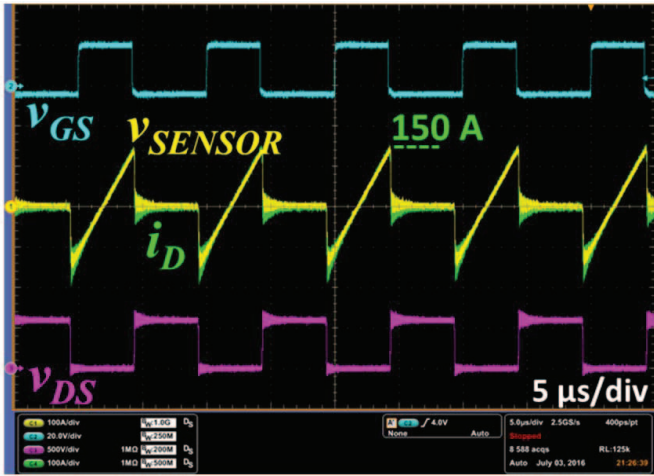


Fig. 24. Sensor performance at continuous Quasi-Square-Wave test

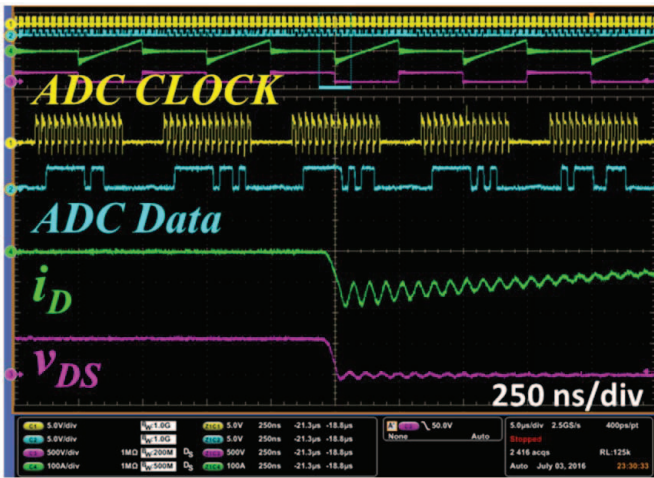


Fig. 25. Sensor performance with digital sampling, sample rate at 2 MHz

V. CONCLUSIONS

A switch current sensor for SiC MOSFET modules is presented in this paper. The sensor is PCB-based and integrated with the gate driver, bringing benefits in both sensor density and cost-effectiveness for mass production. PCB-based shield has been developed to improve the sensor accuracy at high dv/dt conditions. The performance of the sensor is validated in both pulse tests and continuous tests. Excellent protection performance and accurate digital sensing results are also confirmed. Overall, the proposed switch current sensor has great potential in medium-voltage high-current applications for both SiC MOSFETs (protection and current control) and also Si IGBTs (current control).

REFERENCES

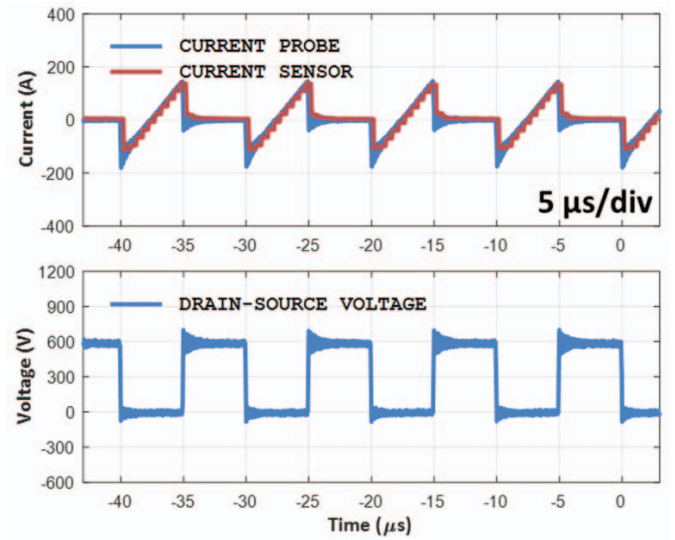


Fig. 26. Comparison between analog and digital waveforms

- [1] J. Millan, P. Godignon, X. Perpina, A. Perez-Tomas, J. Rebollo, "A survey of wide bandgap power semiconductor devices," IEEE Trans. Power Electron., vol. 29, no. 5, pp. 2155-2163, May, 2014.
- [2] J. Wang, Z. Shen, R. Burgos and D. Boroyevich, "Design of a high-bandwidth Rogowski current sensor for gate-drive shortcircuit protection of 1.7 kV SiC MOSFET power modules," Wide Bandgap Power Devices and Appl., IEEE 3rd Workshop on, Blacksburg, VA, 2015, pp. 104-107.
- [3] B. Pelly, "Current Sensint Circuit for Pulse Width Modulated Motor Drive," United State Patent US5815391.
- [4] D. Bortis, J. Biela, and J. W. Kolar, "Active Gate Control for Current Balancing of Parallel-Connected IGBT Modules in Solid-State Modulators," IEEE Trans. Plasma Science, vol. 36, no. 5, pp. 2632-2637, Oct. 2008.
- [5] J. Wang, Z. Shen, R. Burgos, and D. Boroyevich, "Gate driver design for 1.7kV SiC MOSFET module with Rogowski current sensor for shortcircuit protection," in Proc. of Applied Power Electron. Conf. and Expo., 2016.
- [6] J. Wang, R. Burgos, D. Boroyevich and Bo Wen, "Power-cell Switching-Cycle Capacitor Voltage Control for the Modular Multilevel Converters," Int. Power Electron. Conf., 2014, pp. 944-950.
- [7] J. Wang, R. Burgos and D. Boroyevich, "Switching-Cycle State-Space Modeling and Control of the Modular Multilevel Converter," IEEE Journal of Emerging and Selected Topics in Power Electron., vol. 2, no. 4, pp. 1159-1170, Dec. 2014.
- [8] J. Wang, R. Burgos and D. Boroyevich, "Switching-Cycle Capacitor Voltage Control for the Modular Multilevel DC/DC Converters," in Proc. of Applied Power Electron. Conf. and Expo., 2015, pp. 377-384.
- [9] J. Wang, B. Yang, J. Zhao, Y. Deng, X. He and X. Zhixin, "Development of a compact 750KVA three-phase NPC three-level universal inverter module with specifically designed busbar," in Proc. of Applied Power Electron. Conf. and Expo., 2010, pp. 1266-1271.
- [10] J. Wang, R. Burgos and D. Boroyevich, "A survey on the modular multilevel converters — Modeling, modulation and controls," in Proc. of Energy Conv. Congress and Expo., 2013, pp. 3984-3991.
- [11] C.R. Hewson and W.F. Ray, "Optimising the high frequency bandwidth and immunity to interference of Rogowski coils in measurement applications with large local dv/dt," in Proc. of Applied Power Electron. Conf. and Expo. (APEC), vol., no., pp.2050-2056, 21-25 Feb. 2010.